



Insights From m6A RNA Methylation: Biomarkers for Diagnosis of Acute Myocardial Infarction

Wenjun Fan^{1,2}, Wenbin Zhao^{1,2}, Renjie Hu^{1,2}, Chen Wei³, Lixian Sun³, Tong Hou^{1,2}, Ran Li^{1,2}, Qinghua Sun^{1,2}, Cuiqing Liu^{1,2}

¹School of Public Health, Zhejiang Chinese Medical University, Hangzhou, 310053, People's Republic of China; ²Zhejiang International Science and Technology Cooperation Base of Air Pollution and Health, Hangzhou, 310053, People's Republic of China; ³Department of Cardiology, The Affiliated Hospital of Chengde Medical University, Chengde, Hebei, 067000, People's Republic of China

Correspondence: Cuiqing Liu, School of Public Health, Zhejiang Chinese Medical University, 548 Binwen Road, Hangzhou, 310053, People's Republic of China, Tel +86 571 86611320, Email liucuiqing@zcmu.edu.cn

Purpose: Acute myocardial infarction (AMI) is a major contributor to death. The purpose of this study is to explore circulating biomarkers for AMI diagnosis from the perspectives of immunological microenvironment and N6-methyladenosine (m6A) RNA methylation regulation.

Patients and Methods: The GSE59867 dataset was used to download platform and probe data for conducting differential analysis of m6A regulators. A diagnostic nomogram was created utilizing the random-forest method and evaluated for predictive power. m6A-related gene patterns were identified, and their immune microenvironment characteristics were analyzed. Peripheral blood samples were obtained for validation in patient-based investigations using RT-qPCR. The association between m6A regulators and clinical parameters was examined via Spearman correlation analysis.

Results: With a predictive nomogram model developed using key m6A regulators, two distinct m6A subtypes were identified, showing significant variations in infiltrating immunocyte abundance. In confirmation of the model prediction, examination of patient blood identified METTL3, WTAP, RBM15, ALKBH5, FTO, and FMR1 as novel circulating biomarkers for AMI diagnosis. METTL3 and FTO were identified as promising biomarkers for AMI given that they showed a positive correlation with left ventricular ejection fraction.

Conclusion: The study identified six m6A regulators as circulating biomarkers for AMI diagnosis and suggested a potential role for m6A-mediated immune cell infiltration in the pathogenesis of AMI.

Keywords: acute myocardial infarction, immune cell infiltration, N6-methyladenosine, diagnosis, biomarker

Introduction

Acute myocardial infarction (AMI) continues to be the primary source of disease burden worldwide.^{1,2} AMI is characterized by reduced oxygen and blood flow leading to ischemic myocardial necrosis.^{3–5} Failure to restore coronary perfusion may result in myocardial injury, leading to myocardium remodeling and potential development of heart failure.⁶ Prompt revascularization/reperfusion procedures could significantly reduce myocardial infarct area.^{7,8} Myocardial ischemia-reperfusion (I/R) injury involves the worsening and speeding up of damage in the myocardium induced by reperfusion after a period of ischemia. This process is partly facilitated by an intensified inflammatory response,⁹ which leads to the involvement of immune cells and subsequently contributes to the AMI development.¹⁰ The immune microenvironment is comprised of various components, including cytokines, molecules, cellular populations, and extracellular matrices, which collectively form an intricate network that regulates the activity of immune cells.^{11,12} A dysregulation of proinflammatory factors can disrupt the balance between adaptive and innate immunity, leading to the immune microenvironment disruption of AMI patients and contributing to poor outcomes.¹³ Although traditional cardiovascular risk regulators and several hematologic inflammatory markers have been linked to AMI,^{14,15} there remains a need to discover novel biomarkers for early AMI diagnosis.

Microarray technology has facilitated the reliable determination of markers through the use of bioinformatics analysis.^{16,17} Recent data has shown that RNA methylation alterations have a remarkable role in cardiovascular illnesses.^{18,19} N6-methyladenosine (m6A) is widely acknowledged as the most prevailing posttranscriptional alteration in eukaryotic cells. It has a crucial function in regulating the progression of diseases.²⁰ The m6A methylation process entails the N6 position of adenosine methylation inside the RNA molecule. This process is controlled by “writers”, “erasers”, and “readers”.²¹ m6A methylation significantly affects mRNA fate, including as splicing, translation, stability, and degradation.²² Disruption of the regulators involved in m6A methylation has been linked to hypertension, diabetes mellitus, and obesity, all of which are established risk factors for AMI.²³ Moreover, m6A methylation has been linked to the control of circadian rhythm, the response of macrophages, and inflammation, suggesting that it might be a promising target for treating cardiometabolic illnesses.²⁴ m6A methylation has been implicated in mediating structural changes the heart failure. Both in vitro and in vivo studies have demonstrated that Methyltransferase-like 3 (METTL3) and Fat mass-and obesity-associated gene (FTO) have correlation with myocardial infarction (MI).^{25,26} Notably, FTO has been shown to enhance cardiac contraction in heart failure post-MI, suggesting the potential to utilize existing pharmaceuticals or novel inhibitors to modulate m6A modification for therapeutic purposes.²⁵ The above evidence is crucial for clinical translation. Despite its close connection to cardiovascular and immune responses, there is a dearth of studies examining the influence of m6A modification on AMI. The correlation between m6A regulators and immunological features in AMI patients is not well comprehended. Hence, we performed a methodical examination of m6A methylation regulators in AMI using the Gene Expression Omnibus (GEO) database. Subsequently, we validated the diagnostic significance of m6A methylation regulators using peripheral blood samples obtained from patients with AMI.

Materials and Methods

Ethics Statement

This work was approved by the Institutional Review Board of the Affiliated Hospital of Chengde Medical University (number: CYFYLL2023237) and conducted following the Declaration of Helsinki. All participants had written informed consent.

Dataset Source

The GSE59867 dataset, which includes 46 control patients (patients diagnosed with a stable coronary artery disease) and 111 patients with AMI, was obtained from the GEO database. This dataset was chosen due to the distinct categorization (patients and controls) and a sample size larger than 100 to ensure reliable analysis. Subsequently, the genebank matrix was transformed into gene names, allowing for the determination of gene expression levels in each sample. The gene expression profiles were normalized using the “limma” package. A total of twenty-six m6A regulators were retrieved.

Differential Gene Expression and Correlation Analysis

We performed a differential gene expression analysis using the Wilcoxon test to compare m6A-related molecules between patients diagnosed with AMI and control individuals. The “reshape2” was utilized to analyze the gene expression profiles, calculating the mean expression value for genes that appeared several times. Genes that were not expressed in all samples were eliminated. The results were displayed using the “pheatmap” and “ggpubr” packages. The circular representation of the chromosomal locations of m6A-related genes was created using the “RCircos” package. The expression associations among m6A regulators were assessed using Spearman correlation analysis. The resulting relationships were graphically shown via the “ggplot2”, “ggpubr”, and “ggExtra” packages.

Development and Validation of a Nomogram

To determine the more significant genes that are differentially expressed in relation to m6A, we performed two models: support vector machine (SVM) and random forest (RF). These models help us identify the main regulators of m6A. The residuals and the area under the receiver operating characteristic curve (AUC) were used to assess the prediction precision of the two models. The model with improved performance and more accuracy was judged by smaller residuals

and bigger AUC values. The RF model was defined as the most appropriate machine learning model for future exploration. The machine learning model was developed using packages such as “caret”, “DALEX”, “ggplot2”, “randomForest”, “kernlab”, and “pROC”.

More precisely, the average rate of error for all m6A regulators was computed, and the ideal number of trees was established by selecting the lowest error during cross-validation. Afterwards, in order to evaluate the significance of the found genes, a RF model was built using the mean decrease in the Gini index. The importance of a gene in the model depended on the values. Genes with significance scores greater than two were chosen as significant m6A regulators. These regulators were subsequently employed in the construction and validation of a nomogram in this study.

The “rms” R package was utilized to construct a nomogram that predicts the occurrence of AMI using the eighteen identified major m6A regulators. In order to verify the accuracy of a diagnostic nomogram, calibration curve was employed to estimate the accuracy and reliability of the predicted values compared to the actual values. Decision curve analysis (DCA) and the clinical impact curve were used to evaluate the clinical usefulness of the model in predicting AMI.

Identification of the Different m6A Patterns

A clustering analysis was performed to detect distinct patterns of m6A alteration in AMI. The ideal number of clusters (K) was identified by the R package “ConsensusClusterPlus”. Samples from the control group were not considered, and only samples from the AMI group were used for further examination of m6A patterns. The ideal K selected by analyzing the consensus matrix heatmap, cumulative distribution function (CDF), and delta area plot. The consensus matrix heatmap represents clustering, with white indicating an inability to cluster and deep blue indicating strong clustering. The most suitable number of clusters was determined using the k-means clustering matrix. This matrix showed a strong connection (deep blue) within categories and a modest association (light blue) across subtypes. In addition, the CDF plot was utilized to identify the optimal value of K at which the CDF reached its peak. The ideal value of the k parameter for the CDF was established by analyzing the gradual decrease in the slope of the CDF curve. The delta area plot illustrates the proportional difference between adjacent K values. The value of k was determined to be 2 when the area under the curve reached a stable condition, indicating the ideal value for K. We determined that the most suitable number for K was 2. The reliability of consensus clustering and the various m6A alteration patterns were confirmed by the implementation of a principal component analysis (PCA) investigation. We also examined the expression of eighteen crucial m6A regulators in different m6A modification patterns.

Assessment of Immune Cell Infiltration

The enrichment score of infiltrating immune cells in each sample was analyzed via the “GSEABase” and “GSVA” R packages through single sample gene set enrichment analysis (ssGSEA). Common samples found in both the m6A cluster and ssGSEA datasets were identified, and the information from these overlapping samples was preserved and merged. The presence of 23 different kinds of immune cells was evaluated in groups with low and high levels of major m6A regulators. In addition, we used Wilcoxon test to examine the immune cells abundance across various m6A modification patterns and the two distinct groups (low vs high group). The study employed Spearman correlation analysis to determine the correlations between core m6A regulators and immune cells.

Study Population and Clinical Data Collection

A total of 64 patients were sequentially recruited between May 2023 and September 2023 at the Affiliated Hospital of Chengde Medical University. The inclusion criteria were inpatients who were diagnosed with AMI based on the European Society of Cardiology guidelines and fourth universal definition of MI.^{8,27} Additionally, all of the patients enrolled underwent coronary angiography and percutaneous coronary intervention. Control group was defined as those who had undergone coronary angiography and had no diagnostic stenosis in the major coronary arteries or their branches. The exclusion criteria included chronic coronary syndromes, coronary artery spasm, blood system diseases, malignant tumors, infectious diseases, severe heart diseases like hypertrophic cardiomyopathy and aortic dissection, severe systemic disease, glucocorticoid therapies within the past 2 months, systemic inflammatory disorders, and chronic kidney disease at stage 3 or higher.

Prior to coronary angiography, blood samples were collected through the radial artery. After extracting RNA and converting it to cDNA, all the samples were kept at a temperature of -20°C . The study team also recorded the demographic and clinical features, along with the clinical risk factors.

Reverse Transcription-Quantitative Real-Time Polymerase Chain Reaction (RT-qPCR)

Prior research developed a diagnostic nomogram based on m6A regulators between AMI and normal controls.^{16,17} Therefore, we have discovered m6A regulators that have frequently been mentioned in past studies and have a strong connection to cardiovascular disorders. The presence of METTL3, Wilms' tumor 1-associated protein (WTAP), RNA-binding motif protein 15 (RBM15), alkylation repair homologue 5 (ALKBH5), FTO, Fragile X mental-retardation protein (FMR1), and insulin-like growth factor 2 mRNA binding protein 1 (IGF2BP1) was identified by RT-qPCR. Total RNA was obtained from human fresh blood samples using RNAprep pure hi-blood kit (DP443, TIANGEN, China). The total RNA was transformed to cDNA through the use of a FastQuant RT Kit with gDNase (KR116, TIANGEN Biotech Corporation, China). RT-qPCR analysis was performed using the PCR machine (Cobas Z 480, Roche, Basel, Switzerland). Each reaction consisted of 2 μL of forward and reverse primer (concentration of 2 μM each), 2 μL of cDNA, 6 μL of RNAase-Free ddH₂O, and 10 μL of 2 \times SuperReal PreMix Plus (FP205, TIANGEN, China). The reactions took place at a temperature of 95°C for a duration of 15 minutes, with a total of 40 cycles. Each cycle consisted of 10s at 95°C , followed by 20s at 60°C , and finally 20s at 72°C .

The primers were purchased from FugenGene Company (Guangzhou, China) and Generalbiol (Anhui, China): METTL3 (HQP015070, GeneCopoeia, USA), forward 5'-TGCTCCTGCCACTCAAGATG-3', reverse 5'-GGCAGAGAGCTTGGAATGGT-3'; WTAP (HQP022953, GeneCopoeia, USA), forward 5'-TGGTAGACCCAGCGATCAAC-3', reverse 5'-AGCATTCGACACTTCGCCAT-3'; RBM15 (General Biosystems, Anhui, China), forward 5'-TCATTGTCCGTGGGTTTGGT-3', reverse 5'-ATAACAGGGTCAGCGCCAAG-3'; FTO (HQP111736, GeneCopoeia, USA), forward 5'-CCCGAACATTACCTGCTGAT-3', reverse 5'-TTGCTTCCAGAAGCTGACCT-3'; ALKBH5 (HQP013831, GeneCopoeia, USA), forward 5'-ACCCTGCTCTGAAACCCAAG-3', reverse 5'-GCCGGTTCTCTTCCTTGTC-3'; FMR1 (HQP005998, GeneCopoeia, USA), forward 5'-CAGCCTGATAGGCAGATTCCA-3', reverse 5'-AACCACCAACAGCAAGGCTC-3'; IGF2BP1 (HQP000777, GeneCopoeia, USA), forward 5'-ATCGGCAACCTCAACGAGAG-3', reverse 5'-GTTTCGATGGCCTTCATCGC-3'. The house-keeping gene employed in this study was GAPDH (HQP006940, GeneCopoeia, USA). The Threshold cycle (CT) values were measured and the results were analyzed using the formula $2^{-(\Delta\text{CT}-0)} = 2^{-\Delta\text{CT}}$ (where ΔCT = CT of the target gene minus CT of the GAPDH gene). The data underwent a log10 transformation to accurately depict the relative mRNA levels.

Statistical Analysis

The statistical analyses were conducted using R software, GraphPad Prism, PASS and SPSS. We employed a Kolmogorov–Smirnov test to analyze continuous variables. Results were showed as the mean \pm standard deviation for variables that followed a normal distribution. For variables with a skewed distribution, the results were displayed as medians (interquartile range). A *t*-test was used in the statistical procedure for parametric data, while a Mann–Whitney *U*-test was used for nonparametric data. Categorical variables are represented numerically as percentages and are compared using a χ^2 test. The Receiver Operating Characteristic (ROC) analysis was employed to ascertain the effectiveness and ideal threshold for m6A regulators. Spearman's rank correlation was explored to analyze the connection between core m6A regulators and clinical factors. Significance was attributed to $P < 0.05$ in both tails.

Results

Differential Expression Analysis

Figure 1 displays a flow chart outlining the structure of our investigation. The study evaluated a total of twenty-six m6A regulators, consisting of fifteen readers, nine writers, and two erasers. The box plot (Figure 2A) and heatmap (Figure 2B) clearly demonstrate significant variations in the expression levels of 18 modulators across groups, including WTAP, RBM15, FTO, ALKBH5, FMR1, and other regulators, as shown by the Wilcoxon test. Figure 2C illustrates the precise

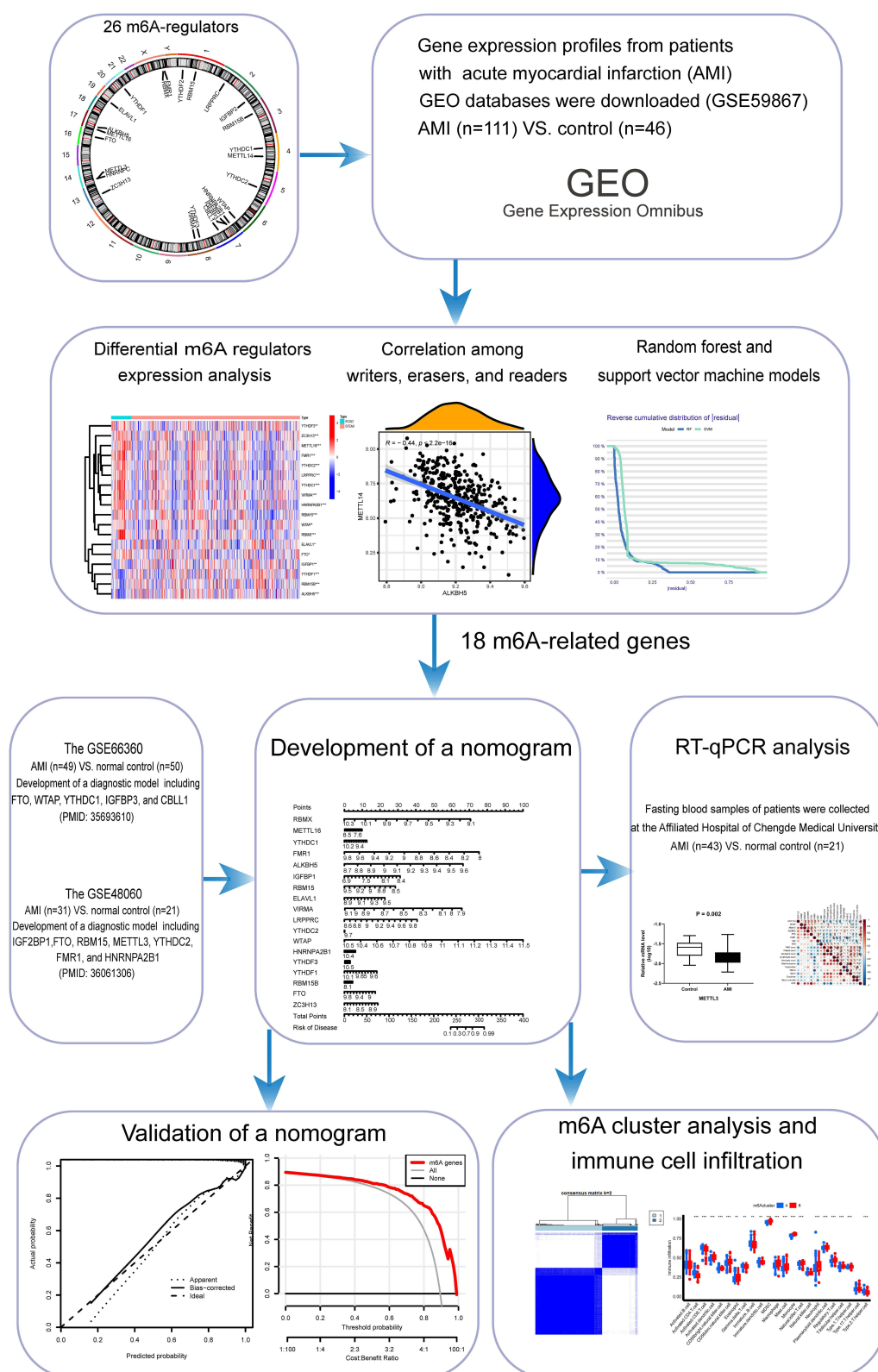


Figure 1 Flow chart of the study.

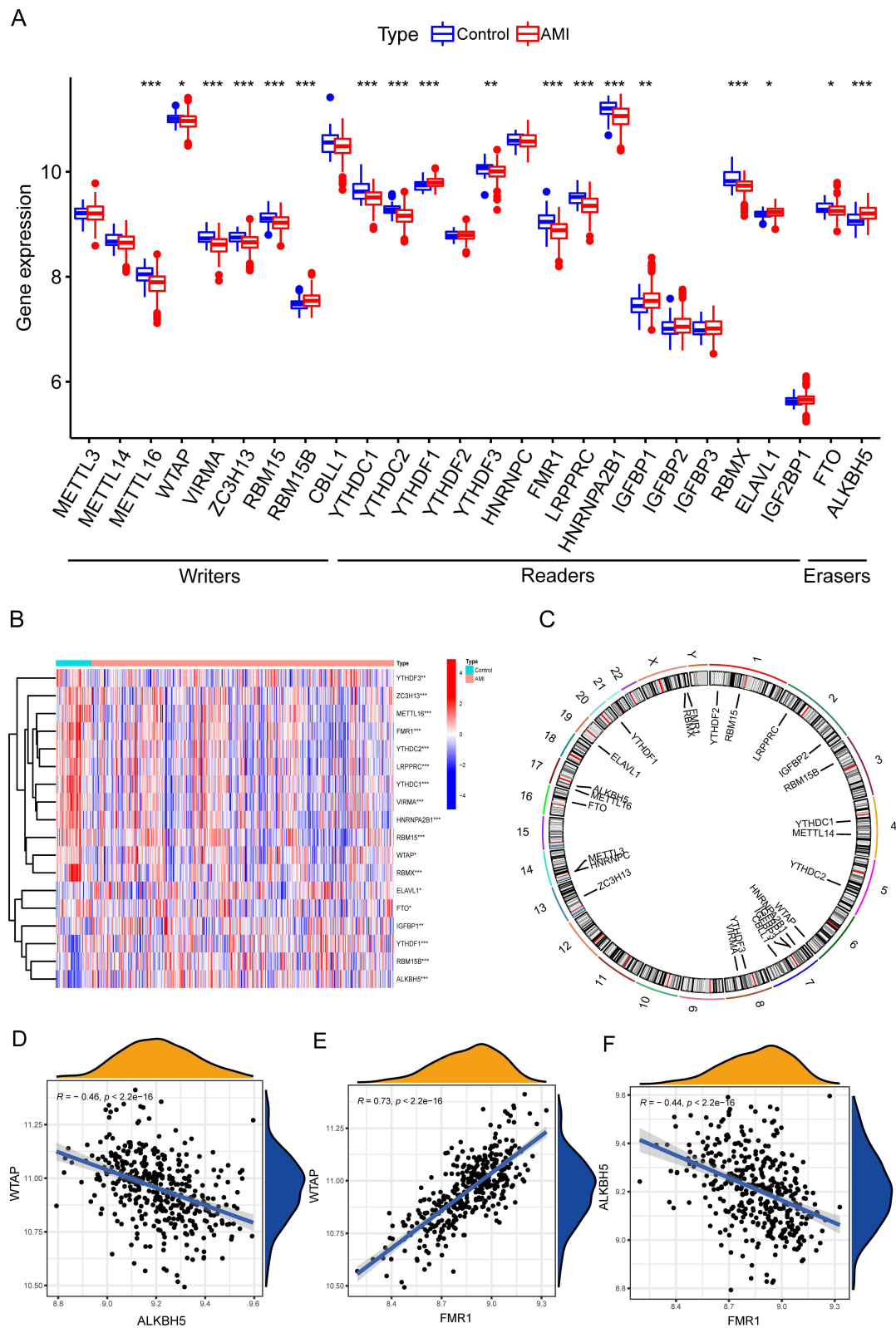


Figure 2 m6A regulators expression and correlation analysis. **(A and B)** Box plot **(A)** and heatmap **(B)** of differentially expressed modulators in two groups. **(C)** The chromosomal location of the m6A modulators. **(D–F)** Correlation of **(D)** WTAP with ALKBH5, **(E)** WTAP with FMR1, and **(F)** ALKBH5 with FMR1. The symbol *, **, *** reveals the value of $P < 0.05$, < 0.01 , and < 0.001 , respectively.

position of the m6A regulators on the chromosome. Later, the connection between the writer, eraser, and reader was examined. There was a significant association seen between WTAP and ALKBH5 ($r = -0.46$), WTAP and FMR1 ($r = 0.73$), ALKBH5 and FMR1 ($r = -0.44$) (Figure 2D–F) (all $P < 0.05$).

Development of the RF and SVM Models

To forecast the occurrence of AMI, we conducted RF and SVM models. An analysis was conducted on the residuals (Figure 3A and B). The RF model exhibited the least residual. The residual observed in the RF model was minimal, suggesting the high efficiency of the model. The AUC for the model created using the RF was 1.000, whereas the AUC for the model created using the SVM was 0.905, as seen in Figure 3C. These findings indicate that the RF approach exhibits more reliability and accuracy in comparison to SVM. Consequently, the RF model was ultimately chosen as the approach for developing the diagnostic model. A total of 150 trees were selected to reduce variability, hence guaranteeing a steady error rate (Figure 3D). Subsequently, as seen in Figure 3E, we selected eighteen crucial m6A regulators with significance ratings greater than two for inclusion in the nomogram model.

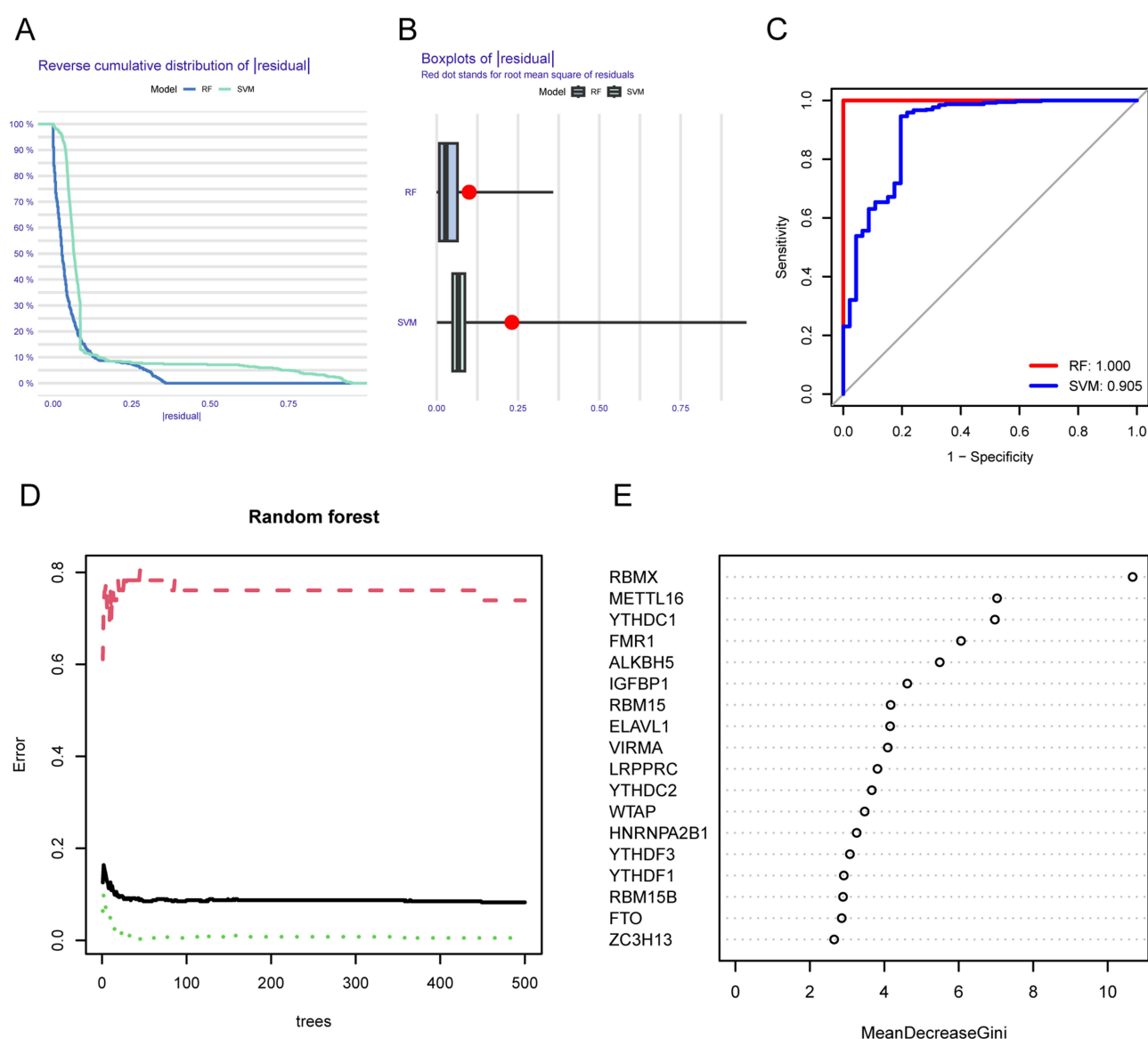


Figure 3 Construction of the RF model to identify the key m6A regulators. (A and B) The residuals of the RF and SVM models. (C) The comparison between the RF and SVM via ROC curves. (D) Error graph of the RF models. (E) The significance of the 18 m6A regulators (MDG value > 2) based on the RF model.

Development and Validation of a Nomogram

A nomogram was created using the eighteen essential m6A regulators to forecast the occurrence rate of AMI (Figure 4A). The nomogram accurately diagnosed AMI, as evidenced by the calibration curve's minimal discrepancy between the anticipated and the actual risks of AMI (Figure 4B). According to the DCA curve, the red line consistently remains higher than the gray and black lines. This suggested that patients with AMI may have more advantages from decisions made through the nomogram (Figure 4C). Figure 4D illustrated two curves: the red curve showed the amount of people identified as high-risk, while the blue curve reflected the number of individuals who are really positive. The nomogram exhibited exceptional capability given that the clinical impact curve was examined.

Identification of Two Different m6A-Related Gene Patterns

We conducted consensus clustering analysis (Figure 5A–C) using the expression levels of regulators. Two m6A patterns (type A and type B) have been determined. The PCA revealed that patients with AMI may be categorized into two distinct groups based on m6A regulators, as seen in Figure 5D. The levels of WTAP, FMR1, RBM15, and FTO were elevated in cluster A compared to cluster B. The levels of ALKBH5 expression in cluster A were comparatively lower compared to cluster B (Figure 5E and F).

Immune Microenvironment Based on Two m6A Patterns

To assess the distinctions in the immune microenvironment between different patterns of m6A modification, we examined the variations in immune cells. The infiltrating immune cells in gene clusters A and B was found to be different (Figure 6A). Furthermore, we assessed the relationship between the eighteen core m6A genes and various immune cells (Figure 6B). We also analyzed the impact of METTL3, WTAP, FTO, and ALKBH5 on immune cell levels in both high- and low-expression groups (Figure 6C–F). These results emphasized the significance of core m6A regulators in the immunological process of AMI.

Basic Characteristics

The patients were categorized into two groups, AMI ($n = 43$) and control ($n = 21$). AMI patients exhibited a greater occurrence of male gender, diabetes, and abnormal wall motion compared to the control group. The AMI group also demonstrated increased levels of white blood cells (WBC) count, monocyte count, neutrophil count, while lower levels of high-density lipoprotein cholesterol (HDL-C) as well as left ventricular ejection fraction (LVEF) (all $P < 0.05$; Table 1).

The Validation of Core m6A Regulators in Peripheral Blood From AMI and Control Patients

m6A regulators consist of three main types: writers, erasers, and readers. In terms of writers, the mRNA levels of METTL3 were decreased in AMI patients, while WTAP levels were elevated in AMI patients ($P < 0.05$, Figure 7A and B). As shown in Figure 7C, the expression of RBM15 was reduced in the group with AMI compared to the control group ($P < 0.05$). The levels of ALKBH5 and FTO erasers were lower in AMI group ($P < 0.05$, Figure 7D and E). Similarly, the expression of FMR1 was significantly reduced in the AMI group ($P < 0.05$, Figure 7F), but no difference was seen in the mRNA levels of IGF2BP1 ($P > 0.05$, Figure 7G).

METTL3 showed a positive association with LVEF, and a negative correlation with the count of WBC and neutrophils. WTAP had a positive correlation with RBM15, which in turn showed positive correlations with ALKBH5, FTO, and LVEF. The FTO gene was found to have a significantly negative correlation with neutrophil count, but a positive correlation with LVEF. FMR1 exhibited a negative correlation with lymphocyte count, monocyte count, and levels of HDL-C (all $P < 0.05$; see Figure 7H).

The AUC and the most effective threshold values for diagnosing AMI using the main m6A regulators METTL3, WTAP, RBM15, ALKBH5, FTO, FMR1, and IGF2BP1, are presented in Table 2. The power of a test showed the power value for METTL3, WTAP, RBM15, ALKBH5, FTO, FMR1, and IGF2BP1 were 0.999, 0.884, 0.790, 0.848, 0.931, 0.950, respectively.

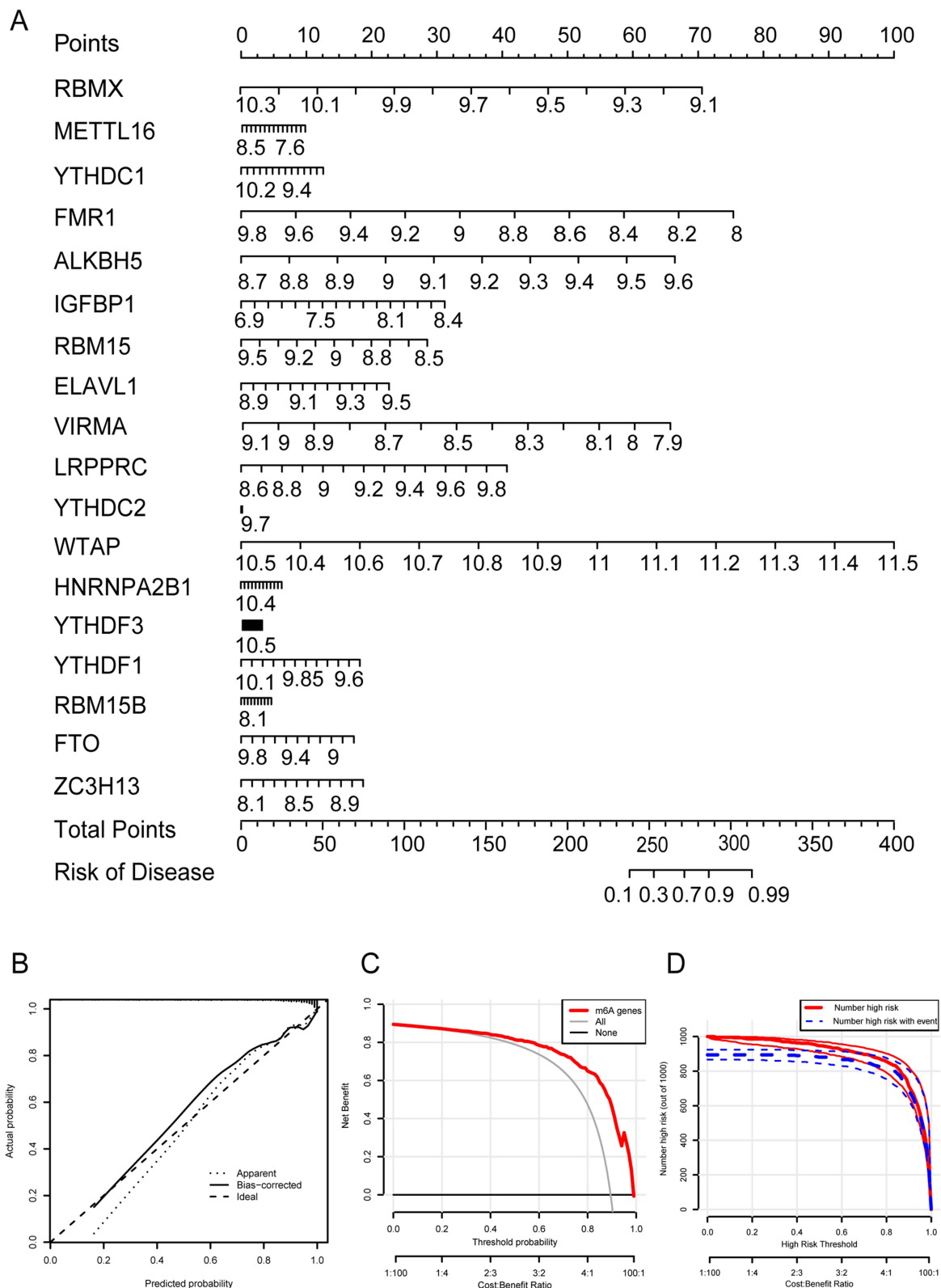


Figure 4 Development and validation of a nomogram of AML. **(A)** The nomogram was built using the 18 key m6A regulators. **(B)** The calibration curve reveals the predictive capacity of the model. **(C)** The DCA indicates that AML patients may have more advantages from decisions made based on the diagnostic nomogram. **(D)** The clinical impact curve reveals that the nomogram has great clinical usefulness.

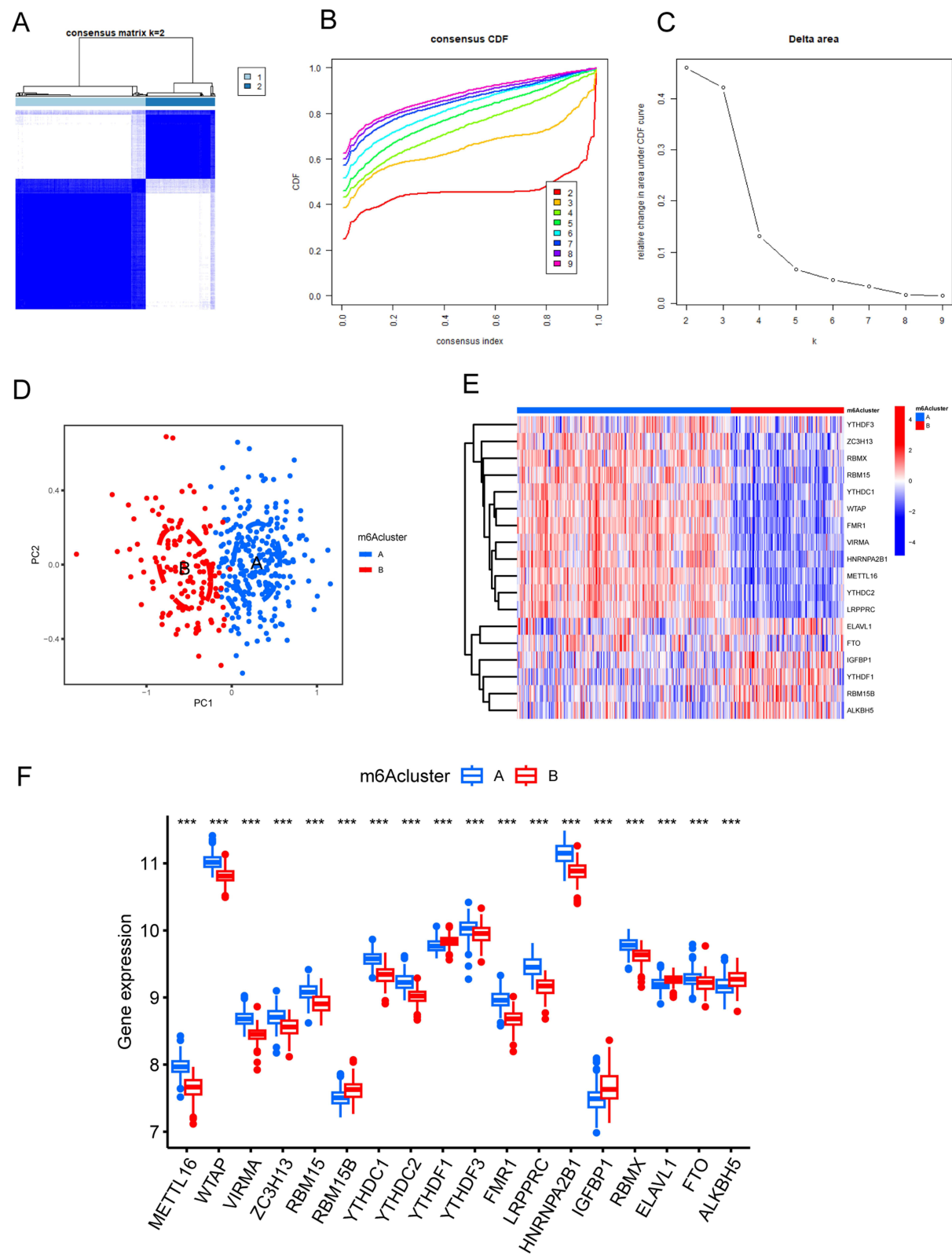


Figure 5 Identification of two different m6A-related patterns. (A) Consensus matrix for 18 core m6A regulators of k=2. (B) Consensus clustering cumulative distribution function for k = 2–9. (C) Delta area variations for k = 2–9. (D) The expression patterns of the 18 core m6A regulators were identified via principal component analysis, which showed remarkable distinctions between two patterns. (E and F) The different expression of 18 m6A regulators between two distinct clusters were shown via the (E) heatmap and (F) box plot. ***P < 0.001.

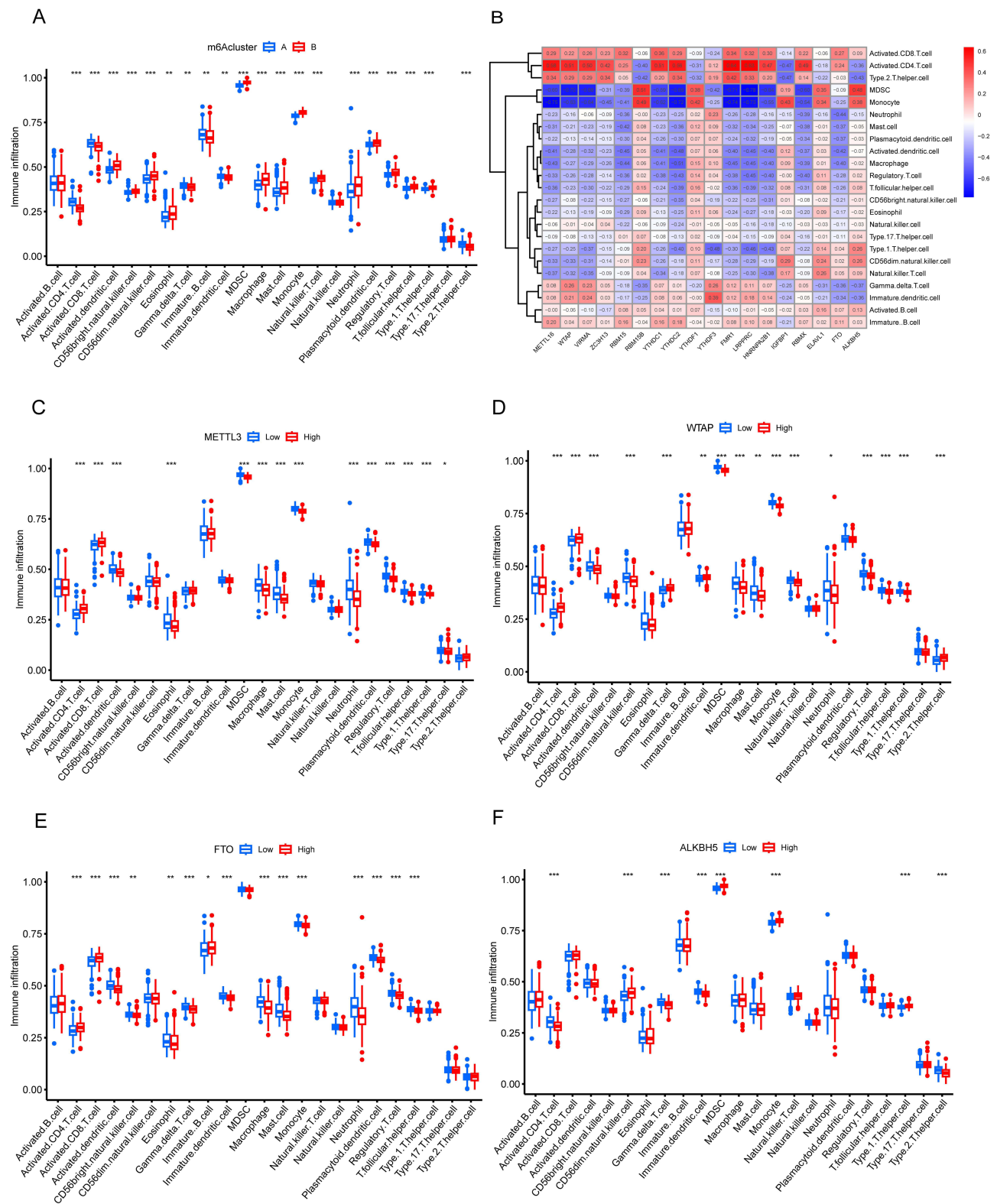


Figure 6 Analysis of immune characteristics among the two different m6A patterns. **(A)** Comparison of infiltrating immune cells in two patterns. **(B)** Correlation between 18 m6A regulators and immune cell abundance. **(C–F)** Distinctions between representative m6A regulator high- and low- level groups. **(C)** High and low METTL3 level. **(D)** High and low WTAP level. **(E)** High and low FTO level. **(F)** High and low ALKBH5 level. The symbol *, **, *** indicates the value of $P < 0.05$, < 0.01 , and < 0.001 , respectively.

Table 1 Baseline Clinical Characteristics of the AMI and Control Groups

Variables	AMI Group (n = 43)	Control Group (n = 21)	$\chi^2 / Z / t$	P-value
Demographic and clinical data, n (%)				
Male sex (%)	35 (81.4)	9 (42.9)	9.754	0.002
Age (years)	55.56 ± 12.46	60.67 ± 6.45	2.160	0.035
BMI (kg/m ²)	25.83(22.90,29.18)	24.60(23.07,28.02)	-0.689	0.491
Time of symptoms before Emergency Department (hours)	11 (4,24)	–	–	–
Smoking (%)	26 (60.5)	8 (38.1)	2.835	0.092
Hypertension (%)	25 (58.1)	10(47.6)	0.630	0.427
Diabetes (%)	16 (37.2)	2 (9.5)	5.350	0.021
Dyslipidemia (%)	32 (74.4)	15 (71.4)	0.065	0.799
Ischemic stroke (%)	8 (18.6)	2 (9.5)	0.883	0.348
Family history of CAD (%)	7(17.1)	2 (9.5)	0.638	0.425
STEMI	28 (65.1)	–	–	–
NSTEMI	15 (34.9)	–	–	–
Laboratory data, M(Q1,Q3)				
WBC count (10 ⁹ /L)	10.15±2.93	5.80 ±1.91	-7.066	<0.001
Platelet count (10 ⁹ /L)	233.24 ±68.89	200.95 ±47.96	-1.924	0.059
Neutrophil count (10 ⁹ /L)	7.65(6.08,10.28)	3.22 (2.31,3.85)	-5.414	<0.001
Lymphocyte count (10 ⁹ /L)	1.66±0.79	1.76 ±0.52	0.505	0.615
Monocyte count (10 ⁹ /L)	0.54 (0.40, 0.64)	0.41 (0.33, 0.46)	-2.901	0.004
Total cholesterol (mmol/L)	4.51 ± 1.15	4.57 ± 1.17	0.190	0.850
Triglycerides (mmol/L)	1.4 (1.1, 2.7)	1.1 (0.7, 1.9)	-0.756	0.449
HDL-C (mmol/L)	1.11 ± 0.28	1.29 ± 0.28	2.168	0.034
LDL-C (mmol/L)	2.87 ± 0.95	2.82 ± 1.07	-0.173	0.863
Creatinine (μmol/L)	62.30 (49.70,79.15)	62.30(49.10,69.78)	-1.406	0.160
Serum uric acid (μmol/L)	361.48 ±140.42	317.08 ±72.74	-1.326	0.190
Cardiac troponin (ng/mL)	14.90 (1.48,24.19)	–	–	–
Echocardiography, n (%)				
LVEDD↑	10 (23.3)	6 (28.6)	0.213	0.645
LVEF	53.30±8.36	63.48±4.84	6.144	<0.001
Abnormal wall motion	30 (69.8)	0 (0)	27.579	<0.001
Coronary angiography, n (%)				
1-vessel disease	7(16.3)	0 (0.0)	-	-
2-vessel disease	12 (27.9)	0 (0.0)	-	-
3-vessel disease	24 (55.8)	0 (0.0)	-	-

Abbreviations: AMI, acute myocardial infarction; BMI, body mass index; CAD, coronary artery disease; STEMI, ST-segment elevation myocardial infarction; NSTEMI, non-ST-segment elevation myocardial infarction; WBC, white blood cell; HDL-C, high-density lipoprotein cholesterol; LDL-C, low-density lipoprotein cholesterol; LVEDD, left ventricular end-diastolic diameter; LVEF, left ventricular ejection fraction.

Discussion

Despite advancements in early diagnosis and intervention of AMI in recent years, it continues to be the dominant cause of death.²⁸ In recent years, m6A modification has garnered attention in various fields and inflammatory diseases, yet there is limited research on m6A methylation specifically in the context of AMI. As far as we know, it is the first study that validated the expression of m6A regulators in AMI and control patients based on previous and current bioinformatics analysis. We found METTL3, WTAP, RBM15, ALKBH5, FTO, and FMR1 could be novel circulating biomarkers for the diagnosis of AMI. Two distinct patterns of AMI patients exhibited significant variations in m6A regulators levels and immune cell abundance, indicating a pivotal role of m6A and the immune microenvironment in the pathogenesis of AMI.

m6A is defined as methylating the 6th N position of adenine, which could regulate diverse biological processes and inflammatory disease development.²¹ Additionally, inflammation has been acknowledged as a crucial factor in the development

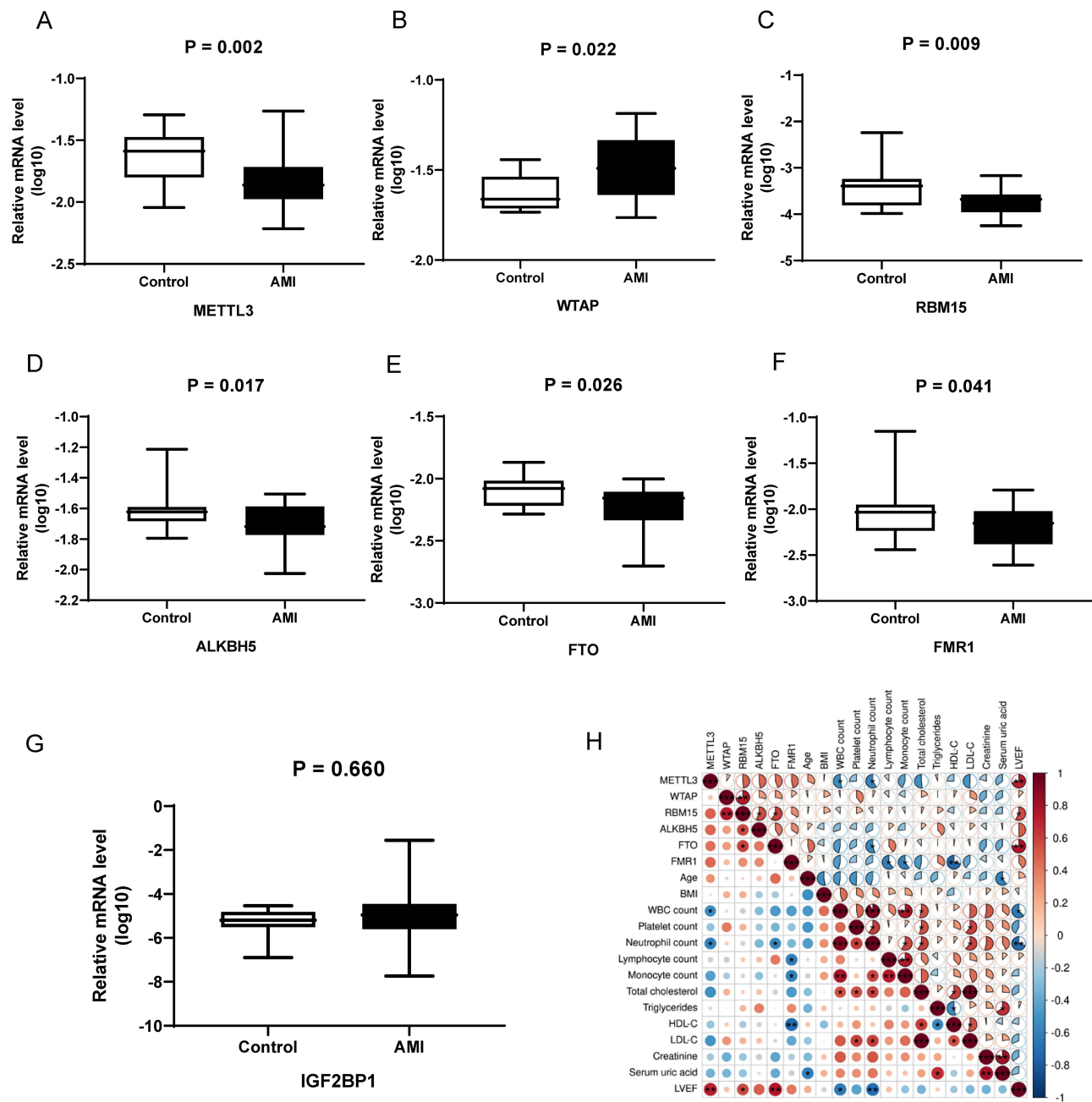


Figure 7 The validation of m6A regulators in peripheral blood from AMI and control patients. (A–G) The expression of core m6A regulators. (A) METTL3, (B) WTAP, (C) RBM15, (D) ALKBH5, (E) FTO, (F) FMR1, and (G) IGF2BP1 mRNA level was detected by RT-qPCR. (H) Correlation heatmap showed the relationship between core m6A regulators and clinical variables.

of AMI.^{29,30} Despite the well-known inflammatory immune response associated with AMI, few studies exploring the involvement of m6A-related immune microenvironment in AMI development. In the present study, a nomogram was developed for diagnosing AMI based on eighteen key m6A regulators. Subsequently, seven m6A regulators were selected based on their consistent appearance in previous studies and their relevance to cardiovascular disease, and peripheral blood samples were collected for further analysis. Our study included 43 patients diagnosed with AMI and 21 control patients. The mRNA expression levels of METTL3, RBM15, ALKBH5, FTO, and FMR1 were found to be lower in the AMI patients, whereas the mRNA level of WTAP was elevated in the AMI patients. Two studies have conducted bioinformatics analyses on existing datasets to examine the global effects of AMI on m6A. Liang et al revealed downregulation of METTL3 and upregulation of WTAP in AMI patients.

Table 2 Receiver Operating Characteristic Curve Analysis of Relative mRNA Level of m6A Factors

Factors	AUC	95% CI	P-value	Se (%)	Sp (%)	Cut off (Log10)
Writers:						
METTL3	0.772	0.626–0.917	0.003	75	75.9	−1.72
WTAP	0.765	0.575–0.955	0.024	71.4	77.8	−1.61
RBM15	0.717	0.563–0.872	0.010	58.8	85.4	−3.51
Erasers:						
ALKBH5	0.689	0.524–0.854	0.044	75.0	68.0	−1.67
FTO	0.714	0.547–0.882	0.028	64.3	76.0	−2.11
Readers:						
FMR1	0.699	0.527–0.870	0.041	73.3	65.2	−2.12
IGF2BP1	0.564	0.336–0.792	0.623	–	–	–

Abbreviations: AUC, area under the curve; CI, confidence interval; Se, sensitivity; Sp, specificity; METTL3, methyltransferase-like 3; WTAP, Wilms’ tumor 1-associated protein; RBM15, RNA-binding motif protein 15; ALKBH5, alkylation repair homologue 5; FTO, Fat mass- and obesity-associated gene; FMR1, fragile X mental retardation 1; IGF2BP1, insulin-like growth factor 2 mRNA-binding protein 1.

Additionally, the FTO and FMR1 were found to be downregulated post-AMI.¹⁶ Wang et al observed downregulation of METTL3, FTO, and FMR1 in AMI patients.¹⁷ Our findings align with previous research on AMI patients, suggesting significant potential for m6A regulators as biomarkers.

Based on the identification of key m6A regulators, our study further revealed m6A-related immune microenvironment variations in AMI patients. The m6A methylation has the potential to affect inflammation, immunity, and metabolism.²⁴ Molecular subtyping strategies are extensively utilized in tumor research, with the discovery of new molecular subtypes aiding in the implementation of more targeted treatments.³¹ Consequently, we effectively classified patients with AMI into two clearly defined groups, which exhibited significant variations in m6A regulators and the presence of immune cells in each subtype. On the one hand, it was observed that the majority of m6A-related genes exhibited higher expression levels in Type A AMI. On the other hand, the presence of activated dendritic cells, natural killer T cells, macrophages, mast cells, monocytes, and neutrophils were found to be elevated in m6A cluster-B. Previous studies have shown that several types of innate immune cells are implicated in AMI.^{11,32,33} Additionally, adaptive immunity, which includes T and B cells, serves as a crucial regulator of AMI.^{11,34} Moreover, we observed the correlations between core m6A regulators and immune cells. Through bioinformatics analysis, we also found decreased levels of METTL3 and FTO with increased levels of macrophages, mast cells, monocytes, and neutrophils. Higher levels of WTAP were associated with increased CD4+ and CD8+ T-cells. Lower expressions of ALKBH5 were linked to higher levels of CD4+ T-cells. The findings mentioned above revealed that m6A-mediated immune cell infiltration is participated in the pathogenesis of AMI.

The novelty and significance lie in the confirmation of the relationship between m6A regulators (writers, erasers, and readers) and clinical parameters in human population. As for writers, METTL3 was observed to have a positive correlation with LVEF and a negative correlation with WBC count and neutrophil count. Additionally, WTAP was positively correlated with RBM15, which in turn was positively correlated with ALKBH5, FTO, and LVEF. Heart failure is a severe complication of AMI.³⁵ Individuals with heart failure are typically categorized based on their LVEF.³⁶ Therefore, the observed positive correlation between METTL3 and WTAP with LVEF highlights their potential associations. METTL3 and WTAP are integral components of m6A writers.³² Recent studies showed that METTL3 played a critical role in regulating macrophage-mediated inflammation and neutrophil activation.^{37,38} The initial observation of METTL3 upregulation was noted in vivo and in vitro, subsequently leading to an elevation in m6A methylation levels.³⁹ Prior research has demonstrated that upregulation of METTL3 is associated with increased inflammation following MI.⁴⁰ Similarly, investigations have been conducted on the m6A writer WTAP, with Wang et al reporting that WTAP contributes to myocardial I/R injury.⁴¹ Taken together, METTL3 and WTAP may contribute to inflammation and serve as potential biomarkers for AMI.

When it comes to erasers, our study identified a positive correlation between FTO and LVEF. The demethylation of m6A is primarily regulated by FTO and ALKBH5.⁴² Consistent with our study, Mathiyalagan et al discovered that decreased FTO expression post-MI leads to hypermethylation in the heart. Overexpression of FTO significantly enhanced cardiac function during the chronic phase post-MI, as evidenced by improved ejection fraction, fractional shortening, and wall motion.²⁵ Studies have indicated that the role of FTO in cardiovascular diseases is different in different cell types, issues, and pathological conditions. Thus, the clinical translation of FTO is likely to require to design tissue-specific or cell-specific agonist or inhibitor.²³ Vausort et al conducted research using a rat model of MI and found that there was an increase in the total levels of m6A in the area affected by the infarction. However, they also detected a drop in m6A levels in the blood samples. Furthermore, a decrease in m6A levels was seen in the peripheral blood samples of MI groups, indicating that blood m6A levels might potentially be considered as an early predictor for worse clinical outcomes after MI.⁴³ The downregulation of ALKBH5 in aged mesenchymal stem cells (AMSCs) has the potential to mitigate cellular senescence and enhance the functionality of AMSCs, thereby augmenting the therapeutic benefits of AMSC-based treatment for MI.⁴⁴ These findings underscore the necessity for further exploration into the participation of FTO and ALKBH5 in the development process of AMI.

In relation to readers, it was found that FMR1 exhibited a negative correlation with lymphocyte count, monocyte count, and levels of HDL-C. Furthermore, research has demonstrated that FMR1 can provide protection to cardiomyocytes against lipopolysaccharide-induced MI.⁴⁵ Gaining a thorough comprehension of the complex control of m6A regulators in the development of AMI is essential for furthering our expertise in this field.

Limitations

It is important to recognize the limitations of this research. First, the underlying mechanisms driving alterations in METTL3, WTAP, RBM15, ALKBH5, FTO, and FMR1 in patients with AMI remain inadequately understood. Second, high-throughput sequencing and other technologies could identify the biological function and chemical basis of m6A, the overall levels of m6A in the peripheral blood of AMI patients may enhance understanding of the diagnostic value of m6A regulators. Third, larger cohorts of AMI patients are needed to validate the results obtained in this study.

Conclusions

Considering the potential m6A regulators, the present study developed a diagnostic nomogram that effectively forecasts the incidence of AMI. Through the validation of this model, novel circulating biomarkers for AMI diagnosis were identified, including METTL3, WTAP, RBM15, ALKBH5, FTO, and FMR1. The study suggested a potential role for m6A-mediated immune cell infiltration in AMI pathogenesis.

Abbreviations

AMI, Acute myocardial infarction; ALKBH5, alkylation repair homologue 5; AUC, the area under the receiver operating characteristic curve; CDF, cumulative distribution function; DCA, Decision curve analysis; FMR1, Fragile X mental-retardation protein; FTO, Fat mass- and obesity-associated gene; GEO, Gene Expression Omnibus; HDL-C, high-density lipoprotein cholesterol; IGF2BP1, insulin-like growth factor 2 mRNA binding protein 1; LVEF, left ventricular ejection fraction; m6A, N6-methyladenosine; METTL3, Methyltransferase-like 3; MI, myocardial infarction; PCA, principal component analysis; RBM15, RNA-binding motif protein 15; RF, random forest; RT-qPCR, Reverse transcription-quantitative real-time polymerase chain reaction; SVM, support vector machine; WTAP, Wilms' tumor 1-associated protein.

Data Sharing Statement

The datasets downloaded in our study are available from GEO (<https://www.ncbi.nlm.nih.gov/geo/>) database, datasets accession number GSE59867. Clinical data will be available on reasonable request.

Acknowledgment

The authors acknowledge that CorrPlot was conducted via the OmicStudio tools at <https://www.omicstudio.cn/tool>.

Funding

This work was supported by National Natural Science Foundation of China (grant number 82273590, 82173480).

Disclosure

The authors declare that they have no competing interests.

References

- Roth GA, Mensah GA, Johnson CO, et al. Global burden of cardiovascular diseases and risk factors, 1990–2019: update from the GBD 2019 study. *J Am Coll Cardiol*. 2020;76(25):2982–3021. doi:10.1016/j.jacc.2020.11.010
- Bergmark BA, Mathenge N, Merlini PA, Lawrence-Wright MB, Giugliano RP. Acute coronary syndromes. *Lancet*. 2022;399(10332):1347–1358. doi:10.1016/S0140-6736(21)02391-6
- Mahmoudi M, Yu M, Serpooshan V, et al. Multiscale technologies for treatment of ischemic cardiomyopathy. *Nat Nanotechnol*. 2017;12(9):845–855. doi:10.1038/nnano.2017.167
- Fox KAA, Metra M, Morais J, Atar D. The myth of “stable” coronary artery disease. *Nat Rev Cardiol*. 2020;17(1):9–21. doi:10.1038/s41569-019-0233-y
- Byrne RA, Rossello X, Coughlan JJ, et al. 2023 ESC guidelines for the management of acute coronary syndromes. *Eur Heart J*. 2023;44(38):3720–3826. doi:10.1093/eurheartj/ehad191
- Algoet M, Janssens S, Himmelreich U, et al. Myocardial ischemia-reperfusion injury and the influence of inflammation. *Trends Cardiovasc Med*. 2023;33(6):357–366. doi:10.1016/j.tcm.2022.02.005
- Collet JP, Thiele H, Barbato E, et al. 2020 ESC guidelines for the management of acute coronary syndromes in patients presenting without persistent ST-segment elevation. *Eur Heart J*. 2021;42(14):1289–1367. doi:10.1093/eurheartj/ehaa575
- Ibanez B, James S, Agewall S, et al. 2017 ESC guidelines for the management of acute myocardial infarction in patients presenting with ST-segment elevation: the task force for the management of acute myocardial infarction in patients presenting with ST-segment elevation of the European Society of Cardiology (ESC). *Eur Heart J*. 2018;39(2):119–177. doi:10.1093/eurheartj/ehx393
- Veltman D, Wu M, Pokreisz P, et al. Clec4e-receptor signaling in myocardial repair after ischemia-reperfusion injury. *JACC Basic Transl Sci*. 2021;6(8):631–646. doi:10.1016/j.jacbs.2021.07.001
- Rai V, Singh H, Agrawal DK. Targeting the crosstalk of immune response and vascular smooth muscle cells phenotype switch for arteriovenous fistula maturation. *Int J Mol Sci*. 2022;23(19):12012. doi:10.3390/ijms231912012
- Roy P, Orecchioni M, Ley K. How the immune system shapes atherosclerosis: roles of innate and adaptive immunity. *Nat Rev Immunol*. 2022;22(4):251–265. doi:10.1038/s41577-021-00584-1
- Rurik JG, Aghajanian H, Epstein JA. Immune cells and immunotherapy for cardiac injury and repair. *Circ Res*. 2021;128(11):1766–1779. doi:10.1161/CIRCRESAHA.121.318005
- Rios-Navarro C, Dios ED, Forteza MJ, Bodi V. Unraveling the thread of uncontrolled immune response in COVID-19 and STEMI: an emerging need for knowledge sharing. *Am J Physiol Heart Circ Physiol*. 2021;320(6):H2240–H2254. doi:10.1152/ajpheart.00934.2020
- Lu Y, Li SX, Liu Y, et al. Sex-specific risk factors associated with first acute myocardial infarction in young adults. *JAMA Netw Open*. 2022;5(5):e229953. doi:10.1001/jamanetworkopen.2022.9953
- Fan W, Wei C, Liu Y, et al. The prognostic value of hematologic inflammatory markers in patients with acute coronary syndrome undergoing percutaneous coronary intervention. *Clin Appl Thromb/Hemost*. 2022;28:10760296221146183. doi:10.1177/10760296221146183
- Liang C, Wang S, Zhang M, Li T. Diagnosis, clustering, and immune cell infiltration analysis of m6A-related genes in patients with acute myocardial infarction—a bioinformatics analysis. *J Thorac Dis*. 2022;14(5):1607–1619. doi:10.21037/jtd-22-569
- Wang X, Wu Y, Guo R, Zhao L, Yan J, Gao C. Comprehensive analysis of N6-methyladenosine RNA methylation regulators in the diagnosis and subtype classification of acute myocardial infarction. *J Immunol Res*. 2022;2022:5173761. doi:10.1155/2022/5173761
- Liu C, Gu L, Deng W, et al. N6-methyladenosine RNA methylation in cardiovascular diseases. *Front Cardiovasc Med*. 2022;9:887838. doi:10.3389/fcvm.2022.887838
- Qin Y, Li L, Luo E, et al. Role of m6A RNA methylation in cardiovascular disease (Review). *Int J Mol Med*. 2020;46(6):1958–1972. doi:10.3892/ijmm.2020.4746
- Tang Y, Chen K, Song B, et al. m6A-Atlas: a comprehensive knowledgebase for unraveling the N6-methyladenosine (m6A) epitranscriptome. *Nucleic Acids Res*. 2021;49(D1):D134–D143. doi:10.1093/nar/gkaa692
- Shi H, Wei J, He C. Where, when, and how: context-dependent functions of RNA methylation writers, readers, and erasers. *Mol Cell*. 2019;74(4):640–650. doi:10.1016/j.molcel.2019.04.025
- Oerum S, Meynier V, Catala M, Tisné C. A comprehensive review of m6A/m6Am RNA methyltransferase structures. *Nucleic Acids Res*. 2021;49(13):7239–7255. doi:10.1093/nar/gkab378
- Zhang B, Jiang H, Dong Z, Sun A, Ge J. The critical roles of m6A modification in metabolic abnormality and cardiovascular diseases. *Genes Dis*. 2021;8(6):746–758. doi:10.1016/j.gendis.2020.07.011
- Xu Z, Lv B, Qin Y, Zhang B. Emerging roles and mechanism of m6A methylation in cardiometabolic diseases. *Cells*. 2022;11(7):1101. doi:10.3390/cells11071101
- Mathiyalagan P, Adamiak M, Mayourian J, et al. FTO-dependent N6-methyladenosine regulates cardiac function during remodeling and repair. *Circulation*. 2019;139(4):518–532. doi:10.1161/CIRCULATIONAHA.118.033794
- Dorn LE, Lasman L, Chen J, et al. The N6-methyladenosine mRNA methylase METTL3 controls cardiac homeostasis and hypertrophy. *Circulation*. 2019;139(4):533–545. doi:10.1161/CIRCULATIONAHA.118.036146
- Thygesen K, Alpert JS, Jaffe AS, et al. Fourth universal definition of myocardial infarction (2018). *Eur Heart J*. 2019;40(3):237–269. doi:10.1093/eurheartj/ehy462
- Reed GW, Rossi JE, Cannon CP. Acute myocardial infarction. *Lancet*. 2017;389(10065):197–210. doi:10.1016/S0140-6736(16)30677-8

29. Bentzon JF, Otsuka F, Virmani R, Falk E. Mechanisms of plaque formation and rupture. *Circ Res*. 2014;114(12):1852–1866. doi:10.1161/CIRCRESAHA.114.302721
30. Stătescu C, Anghel L, Tudurachi BS, Leonte A, Benchea LC, Sascău RA. From classic to modern prognostic biomarkers in patients with acute myocardial infarction. *Int J Mol Sci*. 2022;23(16):9168. doi:10.3390/ijms23169168
31. Li B, Cui Y, Nambiar DK, Sunwoo JB, Li R. The immune subtypes and landscape of squamous cell carcinoma. *Clin Cancer Res*. 2019;25(12):3528–3537. doi:10.1158/1078-0432.CCR-18-4085
32. Libby P, Lichtman AH, Hansson GK. Immune effector mechanisms implicated in atherosclerosis: from mice to humans. *Immunity*. 2013;38(6):1092–1104. doi:10.1016/j.immuni.2013.06.009
33. Cai S, Zhao M, Zhou B, et al. Mitochondrial dysfunction in macrophages promotes inflammation and suppresses repair after myocardial infarction. *J Clin Invest*. 2023;133(4):e159498. doi:10.1172/JCI159498
34. Woodell-May JE, Sommerfeld SD. Role of inflammation and the immune system in the progression of osteoarthritis. *J Orthop Res*. 2020;38(2):253–257. doi:10.1002/jor.24457
35. Sulo G, Sulo E, Jørgensen T, et al. Ischemic heart failure as a complication of incident acute myocardial infarction: timing and time trends: a national analysis including 78,814 Danish patients during 2000–2009. *Scand J Public Health*. 2020;48(3):294–302. doi:10.1177/1403494819829333
36. Mele D, Andrade A, Bettencourt P, Moura B, Pestelli G, Ferrari R. From left ventricular ejection fraction to cardiac hemodynamics: role of echocardiography in evaluating patients with heart failure. *Heart Fail Rev*. 2020;25(2):217–230. doi:10.1007/s10741-019-09826-w
37. Song B, Zeng Y, Cao Y, et al. Emerging role of METTL3 in inflammatory diseases: mechanisms and therapeutic applications. *Front Immunol*. 2023;14:1221609. doi:10.3389/fimmu.2023.1221609
38. Li Q, Yu L, Gao A, et al. METTL3 (Methyltransferase Like 3)-dependent N6-methyladenosine modification on Braf mRNA promotes macrophage inflammatory response and atherosclerosis in mice. *Arterioscler Thromb Vasc Biol*. 2023;43(5):755–773. doi:10.1161/ATVBAHA.122.318451
39. Zhang Y, Hua W, Dang Y, et al. Validated Impacts of N6-methyladenosine methylated mRNAs on apoptosis and angiogenesis in myocardial infarction based on MeRIP-Seq analysis. *Front Mol Biosci*. 2021;8:789923. doi:10.3389/fmolb.2021.789923
40. Qi L, Wang Y, Hu H, et al. m6A methyltransferase METTL3 participated in sympathetic neural remodeling post-MI via the TRAF6/NF-κB pathway and ROS production. *J mol Cell Cardiol*. 2022;170:87–99. doi:10.1016/j.yjmcc.2022.06.004
41. Wang J, Zhang J, Ma Y, et al. WTAP promotes myocardial ischemia/reperfusion injury by increasing endoplasmic reticulum stress via regulating m6A modification of ATF4 mRNA. *Aging*. 2021;13(8):11135–11149. doi:10.18632/aging.202770
42. Deng X, Su R, Weng H, Huang H, Li Z, Chen J. RNA N6-methyladenosine modification in cancers: current status and perspectives. *Cell Res*. 2018;28(5):507–517. doi:10.1038/s41422-018-0034-6
43. Vausort M, Niedolisteck M, Lumley AI, et al. Regulation of N6-methyladenosine after myocardial infarction. *Cells*. 2022;11(15):2271. doi:10.3390/cells11152271
44. Gao X, Liang X, Liu B, et al. Downregulation of ALKBH5 rejuvenates aged human mesenchymal stem cells and enhances their therapeutic efficacy in myocardial infarction. *FASEB J*. 2023;37(12):e23294. doi:10.1096/fj.202301292R
45. Bao J, Ye C, Zheng Z, Zhou Z. Fmr1 protects cardiomyocytes against lipopolysaccharide-induced myocardial injury. *Exp Ther Med*. 2018;16(3):1825–1833. doi:10.3892/etm.2018.6386

Journal of Inflammation Research

Publish your work in this journal

The Journal of Inflammation Research is an international, peer-reviewed open-access journal that welcomes laboratory and clinical findings on the molecular basis, cell biology and pharmacology of inflammation including original research, reviews, symposium reports, hypothesis formation and commentaries on: acute/chronic inflammation; mediators of inflammation; cellular processes; molecular mechanisms; pharmacology and novel anti-inflammatory drugs; clinical conditions involving inflammation. The manuscript management system is completely online and includes a very quick and fair peer-review system. Visit <http://www.dovepress.com/testimonials.php> to read real quotes from published authors.

Submit your manuscript here: <https://www.dovepress.com/journal-of-inflammation-research-journal>

Dovepress
Taylor & Francis Group